Journal Pre-proof

Insight into the photochemistry of atmospheric oxalate through hourly measurements in the northern suburbs of Nanjing, China

Chunyan Zhang, Chi Yang, Xiaoyan Liu, Fang Cao, Yan-lin Zhang

PII: S0048-9697(20)30926-8

DOI: https://doi.org/10.1016/j.scitotenv.2020.137416

Reference: STOTEN 137416

To appear in: *Science of the Total Environment*

Received date: 29 September 2019

Revised date: 16 February 2020

Accepted date: 17 February 2020

Please cite this article as: C. Zhang, C. Yang, X. Liu, et al., Insight into the photochemistry of atmospheric oxalate through hourly measurements in the northern suburbs of Nanjing, China, *Science of the Total Environment* (2020), https://doi.org/10.1016/j.scitotenv.2020.137416

Insight into the photochemistry of atmospheric oxalate through hourly measurements in the northern suburbs of Nanjing, China

Chunyan Zhang[a, ‡], Chi Yang[a, ‡], Xiaoyan Liu[a], Fang Cao[a], Yan-lin Zhang[a, *]

[a] **Yale-NUIST Center on Atmospheric Environment, International Joint Laboratory on Climate and Environment Change (ILCEC), College of Applied Meteorology, Nanjing University of Information Science and Technology, Nanjing 210044, China**

Corresponding author: Yan-Lin Zhang (dryanlinzhang@outlook.com or zhangyanlin@nuist.edu.cn)

‡ equal contribution to the paper

Abstract

Oxalate-iron is an integral part of the photochemical system in the atmosphere. Here, we combined high-resolution online observations and laboratory simulations to discuss the distribution of oxalate and oxalate-iron photochemical system in Nanjing atmosphere at the molecular level. The results show that the oxidation state of iron in the oxalate-iron photochemical system changes significantly and regularly. Among them, Fe (II) / Fe (III) is 3.82 during the day and 0.76 at night. At the same time, Cl^- may accelerate the generation of hydroxyl radicals in the system and promote the photooxidation rate of oxalate. Oxalate can be converted into formate (C1) and acetate (C2) in the photochemical system, but less than 4% of degraded oxalate is converted, which means that the photochemical system may not be the main source of formate and acetate in the atmosphere. Besides, the ratio of C1 / C2 < 1 in the conversion is opposite to the ratio of C1 / C2 > 1 in the general secondary conversion, which means that not all ratio of C1 / C2 in the photochemical pathway is greater than 1. These results are beneficial for us to understand the effect of the oxalate-iron photochemical system on the distribution of oxalate in the atmosphere, and also help us to analyze the conversion of organics in the atmospheric aqueous phase.

Keywords: Oxalate, Fe(II)/Fe(III), Chloride, Formate, Photochemical reaction

1 Introduction

Oxalic acid and oxalate are important components of water-soluble organics in the atmosphere (*Yang et al.*, 2014). They are highly water-soluble so that they can change the properties of oxalate-containing particles, including their hygroscopicity,

size, and cloud condensation nodules (CCN) characteristics (*Feng et al*., 2012). Also, they play a vital role in the formation of new particles and the solubility of iron (*Paris et al*., 2011; *Yang et al*., 2009). Even their photooxidation product, formate, can cause the acidification of water and soil (*Krug and Frink*, 1983). Oxalic acid and oxalate are present in the gas phase, aqueous phase, and aerosol particles, with the highest concentration in the particle phase (*Guo et al., 2016; Laongsri and Harrison*, 2013). The concentration of them in the atmosphere ranges from 10 $ng \cdot m^{-3}$ in remote areas to hundreds or even greater than 1000 $ng \cdot m^{-3}$ in urban areas (*Meng et al*., 2014). Also, their concentration varies greatly in different regions and seasons (*Bian et al*., 2014; *Jiang et al*., 2014; *Meng et al*., 2013; *Pavuluri et al*., 2018; *Wang et al*., 2007; *Zhou et al*., 2015). Among them, the oxalate concentration of inland cities (*Wang et al*., 2007), coastal cities (*Huang et al*., 2006), near-surface marine (*Turekian et al*., 2003), and alpine areas (*Meng et al*., 2013) is decreasing. At the same time, the concentration of oxalate is usually higher during the day than that at night (*Cheng et al*., 2015), and higher in summer than that in winter (*Jiang et al*., 2014; *Pavuluri et al*., 2018). Moreover, they are present in particles of various sizes (*Turekian et al*., 2003), especially in coarse particles (*Huang et al*., 2006; *Martinelango et al*., 2007; *Wang et al*., 2007). These studies indicate the importance and complexity of the distribution of oxalate in the atmosphere.

The cause of the distribution of oxalate in the atmosphere, in addition to the emissions of automobile exhaust (*Kawamura and Kaplan*, 1987) and biomass burning (*Cao et al*., 2017; *Wang et al*., 2007), photochemical oxidation of organics is also an

important source (*Yu et al*., 2005), which has been proved by isotopic analysis (*Kawamura and Watanabe*, 2004; *Pavuluri et al*., 2018; *Turekian et al*., 2003; *Zhang et al*., 2016) and confirmed by field observations (*Bian et al*., 2014; *Cheng et al*., 2015; *Feng et al*., 2012; *Guo et al*., 2016; *Huang et al*., 2006; *Jiang et al*., 2014; *Kawamura and Kaplan*, 1987; *Laongsri and Harrison*, 2013; *Martinelango et al*., 2007; *Meng et al*., 2013; *Meng et al*., 2014; *Paris et al*., 2011; *Turekian et al*., 2003; *Wang et al*., 2007; *Yang et al*., 2009; *Yu et al*., 2005; *Zhou et al*., 2015).The photochemical oxidation can affect not only the formation of oxalate, but also its elimination. Laboratory simulations have confirmed that precursors (*Carlton et al*., 2006; *Chan et al*., 2014; *Guo et al*., 2016; *Kawamura and Bikkina*, 2016; *Kawamura and Kaplan*, 1987; *Kawamura et al*., 1996; *Lim et al*., 2005; *Thomas et al*., 2016; *Warneck*, 2003) such as glyoxal can achieve oxalate formation through the photooxidation system by O_3 photolysis (*He et al*., 2011) or Fenton reaction (*Johnson and Meskhidze*, 2013; *Mangiante et al*., 2017; *Pozdnyakov et al*., 2008; *Vaisi-Raygani et al*., 2007; *Zuo and Hoigne*, 1992). In recent years, the influence of the photooxidation system composed of iron and oxalate on the distribution of oxalate in the atmosphere has received widespread attention (*Cheng et al., 2017; Passananti et al., 2016; Pavuluri and Kawamura, 2012; Sorooshian et al., 2013; Weller et al*., 2014; *Zhang et al*., 2017; *Zhang et al*., 2018). Laboratory simulations of oxalate photooxidation indicate that the reaction forms hydroxyl radicals under the light and the participation of iron, leading to the elimination of oxalate (*Zuo and Hoigne*, 1992). At the same time, laboratory simulations show that the photooxidation system of

oxalate and iron is affected by chemicals such as sulfur dioxide (*Weller et al*., 2014) and malonate (*Wang et al*., 2010). Besides, it is interesting that laboratory simulations suggest that the oxalate-iron intermediate in the photochemical system can also help generate hydroxyl radicals during O_3 photooxidation (*Beltrán et al*., 2005; *Zhang and Croué*, 2014). Also, the field observations have confirmed that oxalate is related to the Fe-containing particles (*Zhou et al.*, 2015; *Zhang et al*., 2018). However, the molecular level of oxalate oxidation in this oxidation system needs to be further understood, and the conversion of oxalate (*Charbouillot et al*., 2012; *Vaïtilingom et al*., 2011; *Yang et al*., 2008) in this photochemical system still needs to be evaluated.

For oxalate in the atmosphere, most existing researches have focused on sampling frequencies of 12h or 24h (*Cao et al*., 2017; *Cheng et al.*, 2015; *Kawamura and Watanabe*, 2004; *Sullivan and Prather*, 2007). However, the half-life of oxalate in the atmosphere is only a few minutes (*Zuo and Hoigne*, 1992), and high-resolution online observations are more conducive to understanding the photochemical process of oxalate in the atmosphere. Based on our previous work (*Cao et al*., 2017; *Zhang et al*., 2016), we used online instrument to analyze the oxalate in the atmosphere with high resolution, and combined simulation experiments to understand the oxalate-iron photochemical system and the distribution of oxalate in the atmosphere at the molecular level. In detail, it includes the change of the iron oxidation state and the conversion of oxalate in this oxalate-iron photochemical system, and the effects of other ions in the atmosphere on this oxalate-iron photochemical system.

.

2 Materials and Methods

2.1 Sampling

The measurements for this study were conducted at an atmospheric observation site on the campus of Nanjing University of Information Science and Technology (NUIST) (32°12′E, 118°42′N), which is located at an altitude of 30 m and surrounded by large enterprises such as energy, chemical, and steel.

Oxalate (particle oxalate was used to represent the oxalate and oxalic acid measured in the atmosphere), and other ions were collected using Gas Components and Aerosol Monitoring systems (MARGA 1S, Metrohm Applikon BV, Netherlands) from March 2016 to February 2017. The description of MARGA can be found elsewhere (*Zhou et al.*, 2015). The system parameters of MARGA are as follows. Anion column and cation columns are Metrosep C4-100 and Metrosep A Supp 10-75, respectively. The water-soluble ions (Na^+, K^+, Ca^{2+}, Mg^{2+}, SO_4^{2-}, NO_3^-, Cl^-, NH_4^+, $C_2O_4^{2-}$) and trace gases (NH_3, HNO_2, HNO_3, HCl, SO_2) can be continuously measured with $1 m^3 \cdot h^{-1}$, due to the faster flow rate, oxalate can be tested in the limited time. The detection limits of water-soluble ions are 0.10 $\mu g \cdot m^{-3}$ for Na^+, 0.08 $\mu g \cdot m^{-3}$ for K^+, 0.08 $\mu g \cdot m^{-3}$ for Ca^{2+}, 0.10 $\mu g \cdot m^{-3}$ for Mg^{2+}, 0.08 $\mu g \cdot m^{-3}$ for SO_4^{2-}, 0.05 $\mu g \cdot m^{-3}$ for NO_3^-, 0.05 $\mu g \cdot m^{-3}$ for Cl^-, 0.08 $\mu g \cdot m^{-3}$ for NH_4^+, and 0.10 $\mu g \cdot m^{-3}$ for oxalate, respectively. Besides, the instrument is calibrated using internal and external standards. The internal standard is a 10 $mg \cdot L^{-1}$ LiBr solution, which is changed every two months. The external standard calibration is performed after replacing the anion and cation columns, and the replacement cycle is generally 2 to 5 months. At the same

time, the MARGA system was cleaned with 1% hydrogen peroxide and 10% acetone solution, and the airflow was calibrated every two months. Formic acid was also observed online at the same time, and its measuring principle is shown below. The air enters the sampling tube at a speed of 16.67 $L \cdot min^{-1}$ after passing through the of the $PM_{2.5}$ cyclone inlet, and then passes through a wet annular denuder. The formic acid in the gas is absorbed by the absorption liquid to form formic acid solution, and then it becomes formate ion in the alkaline eluent, and enters the anion chromatography column to realize the on-line analysis of formate. The above description can be seen elsewhere (*Xu et al*., 2019).

$PM_{2.5}$ was monitored using an asynchronous particle mixing detector (TEOM 1405-DF, Thermo Scientific, MA, USA) coupled to a semi-continuous OC-EC field analyzer system (RT-3131, Sunset Laboratory, OR, USA). Elemental carbon (EC) and organic carbon (OC) were quantified by thermal/optical transmittance methods (Sunset Lab).

Other meteorological data can be obtained from Nanjing Meteorological Station. All parameters are reported as hourly averages, except OC and EC data measured once per hour.

3. Results and discussion

3.1 The distribution of oxalate in the atmosphere

The temporal variations of the temperature (T), relative humidity (RH), precipitation, and the concentrations of $PM_{2.5}$, and water-soluble ions are illustrated in Fig. 1. Precipitation affected the transportation and dissipation of atmospheric

particulate matters, including oxalate. During sampling, the concentration of $PM_{2.5}$ was directly proportional to the concentrations of water-soluble ions (See Table S1 for the average concentrations and concentration ranges of ions). Except for SO_4^{2-}, NO_3^-, and NH_4^+, the concentration of remaining water-soluble ions, including oxalate, gradually increased from spring, summer to winter. RH and T had opposite trends and had different influences on oxalate in three seasons (Fig. S1). Among them, the mass concentration of oxalate in spring rose with the increase of temperature, but it rose first and then decreased with the increase of RH, while in summer, except for the range of 18-23 °C, and it increases first and then decreased in response to the RH. In winter, the effect of temperature is the same as that in spring, but the effect of RH showed no apparent trend, which was different from spring and summer. In general, the concentration of oxalate was related to the increasing temperature and RH of 40-60%, indicating that high temperature and moderate humidity are favorable for the formation of oxalate. The concentration of oxalate was 10.90% higher in summer at 18-23 °C (night) than that at 23-28 °C (daytime), which may be due to the different photochemical reaction environment during the day and night. Among them, at night, the oxalate-iron photooxidation system does not work without sunlight, and fewer hydroxyl radicals are generated, so less oxalate is degraded, resulting in a relatively high oxalate concentration at night (*Kawamura and Yasui*, 2005). Also, the concentration of the oxidant (such as O_3, see Fig. 2) and temperature in summer were higher than those in spring and winter, so oxalate is mainly photooxidized after sunrise in summer.

Fig. 1

The average concentration of oxalate in the sampling period was 0.66 ± 0.31 μg·m^{-3}, which reached the maximum in May (2.12 μg·m^{-3}) and the minimum in July (0.50 μg·m^{-3}) (Fig. S2a). The average seasonal concentration of oxalate was 0.79 ± 0.31 μg·m^{-3} in spring, 0.64 ± 0.27 μg·m^{-3} in summer and 0.51 ± 0.27 μg·m^{-3} in winter. The annual average concentration of oxalate in the northern suburbs of Nanjing was lower than that in the Lahar region of Pakistan (0.97 ± 0.4 μg·m^{-3}) (*Biswas et al.*, 2008), but comparable to that in the northern vicinity of Beijing (607 ± 398 ng·m^{-3}) (*He et al.*, 2014). To our surprise, the concentration of oxalate was higher than that in Nanjing in 2001 (0.22-0.299 ng·m^{-3}) (*Yang et al.*, 2005), which may be due to economic development and population increase over time. In general, the oxalate concentration in the northern suburbs of Nanjing in this study were higher than those previously reported in various cities, suburbs (*He et al.*, 2014), and coasts (*Yang et al.*, 2005), except the Lahar region of Pakistan (*Biswas et al.*, 2008). The concentration of oxalate was successively decreasing from spring through summer to winter (Fig. S2), which is consistent with *Kundu*'s discovery that the concentration of oxalic acid in summer aerosols (564.4 ng·m^{-3}) on Jeju Island in South Korea is higher than that in winter (349.2 ng·m^{-3}) (*Kundu et al.*, 2010). They believe that the difference is due to the relatively strong photochemical reactions in summer. However, in our study, summer and winter are almost not much different, probably because the photochemical production pathway of oxalate in summer is offset by increased wet precipitation (*Zhou et al.*, 2015), so the oxalate concentration

difference between two seasons is not very large. A similar phenomenon existed in the field observations of Aveiro, Portugal, from 2002 to 2004 (*Legrand et al.*, 2007), which also can be explained by the increase of oxalate in summer caused by photochemical activities of the aqueous-phase in the atmosphere.

Fig. 2

The diurnal variation in the concentration of O_3, OC, EC, Cl^-, SO_4^{2-}, NO_3^-, and NH_4^+ may further reveal the characteristics of the oxalate distribution in each season. As shown in Fig. 2, there was a pronounced diurnal variation of OC and oxalate in summer and winter. The changes in summer may be caused by photooxidation of precursors and aqueous-phase reactions, which were reflected in high ambient temperature and RH, and the influence of oxidant (O_3). Similarly, the changes in winter may be caused by photooxidation of precursors with the large consumption of OC during the day (*Zhou et al.* 2015). Relative to the variation of oxalate, the concentration of gas-phase O_3 showed the opposite trend, especially in the summer morning, indicating that O_3 as a catalyst played a vital role in the photochemical reaction of oxalate (*He et al.*, 2011; *Kawamura et al.*, 2005). Also, inorganic ions, such as Cl^-, SO_4^{2-}, NO_3^-, NH_4^+, had opposite diurnal variation with oxalate, they could have influences on the formation and elimination of oxalate as a catalyst or inhibitor (*Dong et al.*, 2007; *Wang et al.*, 2010; *Weller et al.*, 2014). During sampling, the trend of correlation between oxalate with Cl^- and O_3 was the same throughout the day, which means they played important roles in the formation or elimination of oxalate. Especially during the daytime, Cl^- and O_3 affect the distribution of hydroxyl radicals

in the atmosphere (*Cheng et al.*, 2015; *Kawamura et al*., 2005; *Kawamura and Kaplan*, 1987; *Turekian et al.*, 2003;), which are non-negligible reasons for the production and consumption of oxalate. Among them, the correlation between oxalate and Cl^- was good from 11:00 to 18:00 in spring (r: 0.50 ~ 0.81, $p < 0.05$), from 9:00 to 20:00 in summer (r: 0.53 ~ 0.92, $p < 0.05$) and from 6:00 to 23:00 in winter (r: 0.31 ~ 0.64, $p < 0.05$) (Fig. S3-S5), indicating that they may have the same source or Cl^- can affect the formation of oxalate during this period. Cl^- generally comes from sea salt, coal, soil, and industrial emissions (*Cheng et al.*, 2017; *Zuo and Hoigne*, 1992). The diurnal variation of Cl^- observed here may be related to the working hours of steel plants near the sampling point. Besides, for hourly correlation between oxalate with Cl^-, the related duration was analyzed (sum of hours when oxalate and Cl^- are correlated). The related duration between oxalate and Cl^- in winter was longer than that in spring and summer (related duration of oxalate and Cl^-, spring: 12 h, summer: 15 h, winter: 18 h), which may be related to winter heating in the northern cities and long-distance secondary aerosol generation. As for the correlation between oxalate and O_3, the general correlation coefficient was between 0.3 and 0.8, which in spring was higher than 0.5 from 10:00 to 19:00 ($p < 0.05$, Fig. S3). In summer (Fig. S4), the correlation between oxalate and O_3 was relatively high from 7:00 to 23:00 and reached 0.8 from 10:00 to 17:00 ($p < 0.05$). The correlation between oxalate and O_3 in winter was relatively low, and it was higher than 0.6 from 13:00 to 19:00, and from 0:00 to 10:00 it was between 0.3 and 0.4 ($p < 0.05$, Fig. S5). The correlation between oxalate and O_3 was low, and related time was shorter in winter than that in spring and

summer (related duration of oxalate and O_3, spring: 23 h, summer: 24 h, winter: 16 h). The difference between winter and summer may come from the duration and intensity of sunlight, which is the essential factor affecting the distribution of oxalate. These high-resolution (1 h) results indicated that Cl^- and O_3 are important factors influencing the photochemical production of oxalate.

3.2 Oxalate-iron photochemical system and the elimination of oxalate

As mentioned above, in recent years, it has been agreed that the oxalate-iron photochemical system has an important influence on the distribution of oxalate in the atmosphere (*Sorooshian et al., 2013; Wang et al., 2010; Weller et al., 2014; Yang et al*., 2009; *Yu et al*., 2005; *Zhang et al*., 2017; *Zhang et al*., 2018). The mechanism of oxalate photochemical degradation in this system has been analyzed and studied in depth (*Mangiante et al*., 2017; *Pozdnyakov et al*., 2008; *Zuo and Hoigne*, 1992). However, the understanding of this mechanism at the molecular level and the corresponding relationship in the field observation remain to be further evaluated. If there is no light, will the oxidation state of iron change, and whether this oxidation system will be affected by other inorganic ions in the atmosphere, especially the conversion of oxalate itself in this oxidation system. These discussions are as follows.

3.2.1 Fe(II)/Fe(III) and Cl^- in oxalate-iron photochemical system

For the laboratory simulation of the oxalate-iron photooxidation system *(Zuo and Hoigne*, 1992), the inferred mechanism is shown in Fig. 3. Oxalic acid and iron ions can form $Fe(C_2O_4)_3^-$ complex, which directly generates Fe^{2+} and $C_2O_4^-$ under

ultraviolet light, and then $C_2O_4^-$ promotes the regeneration of hydroxyl radicals. During this process, the ability of H_2O_2 to decompose into hydroxyl radicals is very weak, but under the catalysis of Fe(II), it can decompose rapidly in large quantities. Meanwhile, Fe (II) and Fe (III) can be continuously converted into each other. Simultaneously, the intermediate oxalate-iron complex can promote the photolysis of ozone and form hydroxyl radicals (*Dong et al*., 2007; *Wang et al*., 2010).

Fig. 3

In our study, the Fe (II) / Fe (III) ratio obtained by in-situ analysis using XPS for the oxidation state of iron in the field observation samples was 3.82 during the day and 0.76 at night in spring (Fig. S6), and the corresponding oxalate concentration was 0.93 $\mu g \cdot m^{-3}$ during the day and 0.89 $\mu g \cdot m^{-3}$ at night. However, Fe (II) and Fe (III) were only be measured in spring day and night samples. In summer and winter samples, Fe (II) was not detected during the day and night, and only weak Fe (III) was detected. This result is also consistent with the result that the Fe (II) in the cloud water sample during the day and night account for 62% and 50% of the total Fe (II) in the whole day, respectively (*Deutsch et al*., 2001). These field observation results also indicated that the change in the oxidation state of iron in the atmosphere was closely related to the photochemistry of oxalate. Most of the iron exists in the form of Fe (II) because of the intense sunlight during the day. In contrast, iron is converted to Fe (III) by hydrogen peroxide during the night (*Deutsch et al*., 2001). In the change of iron oxidation, the oxalate-iron oxidation system significantly affects the formation and elimination of oxalate in the atmosphere, including dissolving different forms of iron in aqueous-phase in the presence of organic acids (*Sorooshian et al*., 2013; *Weller et*

al., 2014). However, there was a lack of correspondence between iron and oxalate, this also indirectly indicated that the oxalate-Fe (III) / UV system does not directly participate in the formation of hydroxyl radicals, rather acts as an intermediate and catalyst, such as synergistic O_3 production hydroxyl radicals (*Beltrán et al*., 2005; *Wang et al*., 2010; *Zhang and Croué*, 2014).

The existing technology cannot achieve high-resolution real-time analysis of changes in the oxidation state of iron, but the determination of the total iron content in single particles has been achieved. Some studies have analyzed that the content of aerosol iron is 60-1144 $ng \cdot m^{-3}$, and dissolved iron accounted for 6.7-26.5%, which is affected by NO_3^- and nss-SO_4^{2-} (*Srinivas et al*., 2014; *Srinivas et al*., 2012). *Zhang et al.* (2018) found that Fe-containing particles mixed with oxalate are 8.7%, 23.1%, 45.2%, and 31.2% from spring to winter. *Zhou et al.* (2015) used a single-particle aerosol mass spectrometer to observe Hong Kong's oxalate-iron particles at high resolution, and the result showed that diurnal variations of oxalate were consistent with the number fraction of iron oxalate particles. Among them, up to 50% of the iron particles coexisted with oxalate at night, but drop sharply after sunrise to become as low as 5% during the day. This observation supported the suggestion that oxalate was rapidly degraded in iron-containing particles under sunlight, and may be present in aqueous-phase in the form of an oxalate-Fe (III) complex at night. Based on these results, some studies have further found that iron-containing oxalate particles are related to humidity. When the relative humidity is higher than 60%, the aerosol water content may play an important role in the formation of oxalate, and the interaction

with iron promotes the diurnal variation of oxalate in the iron-containing particles (*Huang et al*., 2018; *Zhang et al*., 2018). Similarly, in our 30 randomly selected samples of atmospheric particulate matter, the iron content in atmospheric particles is highest in spring (Fig. S7a), followed by winter and lowest in summer (Fig. S7b and S7c), and that in spring and summer nights was slightly higher than that during the day. Corresponding to changes in oxalate, these results reconfirmed the important role of iron in the oxalate-iron photochemical system.

In addition, some studies have shown that many factors can affect the generation of hydroxyl radicals in the oxalate-iron photooxidation system, which in turn affects the degradation of oxalate in this oxidation system. These factors include metal ions such as iron and copper (*Sedlak et al*., 1997; *Sorooshian et al*., 2013; *Takahama et al*., 2008; *Weller et al*., 2014) and pH (*Joonseon and Jeyong*, 2005). In addition, laboratory simulations show that Cl^- can participate in the valence transition of iron to form chlorine radicals, which help generate more hydroxyl groups and accelerate the oxidative degradation of oxalate, as described below (Eqs.1-5, *Dong et al.*, 2007). At present, it is considered that chlorine-free radicals are involved in the photochemical degradation of organics in the atmosphere. However, through laboratory simulations of Cl^- participating in the oxalate-iron photochemical system, we found that Cl^- may accelerate the photooxidative degradation of oxalate (Fig. S12), which may also be the involvement of Cl^- to generate more hydroxyl radicals in the oxalate-iron system (*Dong et al*., 2007). At the same time, in the field observation, Cl^- form free radicals to participate in the photooxidation of organics (*Ifang et al*., 2015). It is not clear

whether it is the chlorine free radical or the cooperative process of Cl^- and oxalate-iron photochemistry. However, it is worth noting that the correlation between Cl^- and oxalate during the day when sampling is higher than that at night, especially in summer (r: 0.53 ~ 0.92, from 9:00 to 20:00). All these show that Cl^- was very likely to participate in the oxalate-iron photochemical process.

$$Fe^{3+}+Cl^- \leftrightarrow \left[Fe(Cl)^{2+}\right] \quad (1)$$

$$\left[Fe(Cl)^{2+}\right] \xrightarrow{h\nu} Fe^{2+}+Cl^{\bullet} \quad (2)$$

$$Fe^{2+}+Cl\bullet \longrightarrow Fe^{3+}+Cl^- \quad (3)$$

$$H_2O+Cl\bullet \longrightarrow H^++ClOH^{\bullet-} \quad (4)$$

$$H^++ClOH^{\bullet-} \longrightarrow Cl^-+HO^{\bullet} \quad (5)$$

3.2.2 Intermediates in oxalate-iron photochemical systems

It is generally believed that the precipitation of oxalate is mainly through rainfall pathways (*Krug and Frink*, 1983), so this largely depends on weather conditions. As can be seen from Fig. S8, oxalate always had the highest concentration during haze days in each season of observation, and during clean weather, the concentration of oxalate was higher in spring than that in winter, but it was the largest in summer. The strong photochemical reactions in summer may lead to higher oxalate concentrations during clean weather. However, during rainy days, compared with haze weather, the concentration of oxalate was significantly reduced regardless of the winter, due to wet deposition, low solar radiation, and reduced release from biological sources (*Meng et al.*, 2014). Further detailed research, as shown in Table S2, we analyzed oxalate concentration of four episodes during the rain period, including water-soluble ion

average mass concentration of 3 h before precipitation, during precipitation, and 3 h after precipitation. Compared with the concentration of oxalate before and after precipitation, about 20% of oxalate is eliminated. At the same time, precipitation has a definite effect on the removal of water-soluble ions, especially for the three main water-soluble ions NO_3^-、SO_4^{2-}、NH_4^+, and the clearance rate of Cl^- was notably more than 80% in the first three episodes. Therefore, precipitation can not only cause the precipitation of oxalate in the atmosphere but also clean the factors that can affect the photooxidation reaction of oxalate. Besides, we have found that oxalate in the atmosphere remains in a range of 0.11-1.07 $\mu g \cdot m^{-3}$ (the typical range for clean weather) even if there is no rainwater precipitation, which indicates that there exist other pathways of oxalate elimination, maybe photochemical degradation.

In our laboratory simulation (see Text S1 for experiment details), similar to succinic acid can produce low molecular acids (*Chan et al*., 2014), oxalate can be converted to formate and acetate in the oxalate-iron photochemical system (Fig. S10 and S11). At the same time, in the field observation, our analysis found that the trend of oxalate and formic acid in the atmosphere has an apparent regularity, and some reported data show a good correlation between oxalate and formate (r = 0.552) and acetate (r= 0.638) *(Tanner and Law*, 2003). So, in the atmosphere, can oxalate be converted to formate and acetate by photooxidation? Unfortunately, only about 1.3% of the oxalate degraded produced formate and 2% for acetate in our simulation experiments. Besides, the sources of formic acid and acetic acid in the atmosphere are also very complicated. These results suggest that oxalate can be converted to formate

and acetate in the oxalate-iron photooxidation system, but it seems that the contribution of this pathway to atmospheric formic acid and acetic acid is not significant.

It is worth noting that the ratio of formate to acetate (C1/C2) is often used to indicate primary and secondary sources of aerosol. Among them, formate mainly comes from secondary sources, such as isoprene oxidation, OH-induced oxidation and ozonolysis of monoterpenes (*Lee et al*., 2006a; *Lee et al*., 2006b; *Millet et al*., 2015). In contrast, acetate is mainly from primary sources, such as automobile exhaust and biomass burning (*Kawamura et al*., 2000; *Wang et al*., 2007). Here, the ratio of C1/C2 converted in the oxalate-iron photooxidation system was <1 (0.78 ± 0.29, Fig. 4 (b)). This is in contrast to C1/C2 > 1 in existing secondary sources (*Boreddy et al*., 2017; *Verma et al*., 2017), which means that not all C1/C2 ratios in secondary sources are consistent, there may be some ＜1, and others ＞1.

Fig. 4

4 Conclusions

Here, the advantages of high-resolution online observations were used to analyze the distribution of atmospheric oxalate in the northern suburbs of Nanjing. The annual average concentration is 0.66 ± 0.31 $\mu g \cdot m^{-3}$. The hourly correlation between SO_4^{2-}, NO_3^- and oxalate indicates that secondary photooxidation has an important effect on the distribution of oxalate in the atmosphere of Nanjing. For the widespread oxalate-iron photochemical system, combined with field observation results, we discussed the understanding of oxalate in this photochemical system at the molecular

level in Nanjing. The results showed that the change of the iron oxidation state had a greater impact on the generation of hydroxyl radicals in the system. Fe(II) was relatively abundant during the day, generating more free radicals to achieve photochemical oxidation of oxalate. At the same time, it was found that this photochemical system was also affected by Cl^- in the atmosphere. Laboratory simulations showed that Cl^- can accelerate the generation of hydroxyl radicals in the oxalate-iron photochemical system, and then accelerate the photooxidation rate of oxalate. However, Cl^- generally can directly participate in the oxidative degradation of organics in the atmosphere with chlorine radicals. Whether it can participate in the oxalate photooxidation in the way above needs further research. Besides, the simulation experiments showed that oxalate can be converted to formate and acetate in the oxalate-iron photochemical system, but less than 4% of the degraded oxalates were involved in the conversion, which means that this conversion pathway might not be the main source of formic acid and acetate in the atmosphere. Surprisingly, the ratio of C1/C2 < 1 in this conversion pathway is opposite to the commonly thought photochemical pathway. These studies are helpful for our deep understanding of the influence of the oxalate-iron photochemical system in the distribution of atmospheric oxalate, also for us to analyze the aqueous-phase photochemical reactions and its contributions in the atmosphere.

Acknowledgments

The authors thank funding support from the National Nature Science Foundation of China (Nos. 41977305 and 41761144056), the Natural Science Foundation of

Jiangsu Province (No. BK20180040), the fund from Jiangsu Innovation & Entrepreneurship Team. Here, we pay high respect to the medical staff who are fighting in the front line of pneumonia.

References

Beltrán, F. J., Rivas, F. J., and Montero-De-Espinosa, R., 2005. Iron type catalysts for the ozonation of oxalic acid in water. Water Research. 39(15), 3553-3564. https://doi.org/10.1016/j.watres.2005.06.018.

Bian, Q., Huang, X. H. H., and Yu, J. Z., 2014. One-year observations of size distribution characteristics of major aerosol constituents at a coastal receptor site in Hong Kong - Part 1: Inorganic ions and oxalate. Atmospheric Chemistry & Physics. 14(14), 1443-1480. https://doi.org/10.5194/acp-14-9013-2014.

Biswas, K. F., Ghauri, B. M., and Husain, L., 2008. Gaseous and aerosol pollutants during fog and clear episodes in South Asian urban atmosphere. Atmospheric Environment. 42(33), 7775-7785. https://doi.org/10.1016/j.atmosenv.2008.04.056.

Boreddy, S. K. R., Mochizuki, T., Kawamura, K., et al., 2017. Homologous series of low molecular weight (C1-C10) monocarboxylic acids, benzoic acid and hydroxyacids in fine-mode (PM2.5) aerosols over the Bay of Bengal: Influence of heterogeneity in air masses and formation pathways. Atmospheric Environment. 167, 170-180. https://doi.org/10.1016/j.atmosenv.2017.08.008.

Cao, F., Zhang, S. C., Kawamura, K., et al., 2017. Chemical characteristics of dicarboxylic acids and related organic compounds in PM2.5 during biomass-burning and non-biomass-burning seasons at a rural site of Northeast China. Environmental Pollution. 231(Pt1), 654-662. https://doi.org/10.1016/j.envpol.2017.08.045.

Carlton, A. G., Turpin, B. J., Lim, H. J., et al., 2006. Link between isoprene and secondary organic aerosol (SOA): Pyruvic acid oxidation yields low volatility organic acids in clouds. Geophysical Research Letters. 33(6), 272-288. https://doi.org/10.1029/2005gl025374.

Chan, M. N., Zhang, H., Goldstein, A. H., et al., 2014. Role of water and phase in the heterogeneous oxidation of solid and aqueous succinic acid aerosol by hydroxyl radicals. Journal of Physical Chemistry C. 118(50), 28978-28992. https://doi.org/10.1021/jp5012022.

Charbouillot, T., Gorini, S., Voyard, G., et al., 2012. Mechanism of carboxylic acid photooxidation in atmospheric aqueous phase: Formation, fate and reactivity. Atmospheric Environment. 56(5), 1-8. https://doi.org/10.1016/j.atmosenv.2012.03.079.

Cheng, C., Li, M., Chan, C. K., et al., 2017. Mixing state of oxalic acid containing particles in the rural area of Pearl River Delta, China: Implications for the formation mechanism of oxalic acid. Atmospheric Chemistry & Physics. 17(15), 9519-9533. https://doi.org/10.5194/acp-17-9519-2017.

Cheng, C., Wang, G., Meng, J., et al., 2015. Size-resolved airborne particulate oxalic and related secondary organic aerosol species in the urban atmosphere of Chengdu, China. Atmospheric Research. 161-162, 134-142. https://doi.org/10.1016/j.atmosres.2015.04.010.

Deutsch, F., Hoffmann, P., and Ortner, H. M., 2001. Field experimental investigations on the Fe(II)- and Fe(III)-Content in cloudwater samples. Journal of Atmospheric Chemistry. 40(1), 87-105. https://doi.org/10.1023/a:1010684628804.

Dong, Y., Chen, J., Li, C., et al., 2007. Decoloration of three azo dyes in water by photocatalysis of Fe (III)–oxalate complexes/H2O2 in the presence of inorganic salts. Dyes & Pigments. 73(2), 261-268. https://doi.org/10.1016/j.dyepig.2005.12.007.

Feng, J. L., Guo, Z. G., Zhang, T. R., et al., 2012. Source and formation of secondary particulate matter in PM2.5 in Asian continental outflow. Journal of Geophysical Research Atmospheres. 117(D3), 1-11. https://doi.org/10.1029/2011JD016400.

Guo, T., Li, K., Zhu, Y., et al., 2016. Concentration and size distribution of particulate oxalate in marine and coastal atmospheres-Implication for the increased importance of oxalate in nanometer atmospheric particles. Atmospheric Environment. 142, 19-31. https://doi.org/10.1016/j.atmosenv.2016.07.026.

He, N., Kawamura, K., Okuzawa, K., et al., 2014. Diurnal and temporal variations of water-soluble dicarboxylic acids and related compounds in aerosols from the northern vicinity of Beijing: Implication for photochemical aging during atmospheric transport. Science of the Total Environment. 499, 154-165. https://doi.org/10.1016/j.scitotenv.2014.08.050.

He, Z., Zhang, A., Li, Y., et al., 2011. Chlorophene degradation by combined ultraviolet irradiation and ozonation. Journal of Environmental Science & Health Part A Toxic/hazardous Substances & Environmental Engineering. 46(1), 1-8. https://doi.org/10.1080/10934529.2011.526065.

Huang, X., Zhang, J., Luo, B., et al., 2018. Characterization of oxalic acid-containing particles in summer and winter seasons in Chengdu, China. Atmospheric Environment. https://doi.org/10.1016/j.atmosenv.2018.10.050.

Huang, X. F., Yu, J. Z., He, L. Y., et al., 2006. Water-soluble organic carbon and oxalate in aerosols at a coastal urban site in China: Size distribution characteristics, sources, and formation mechanisms. Journal of Geophysical Research Atmospheres. 111(D22). https://doi.org/10.1029/2006jd007408.

Ifang, S., Benter, T., and Barnes, I., 2015. Reactions of Cl atoms with alkyl esters: kinetic, mechanism and atmospheric implications. Environmental Science & Pollution Research. 22(7), 4820-4832. https://doi.org/10.1007/s11356-014-2913-9.

Jiang, Y., Zhuang, G., Wang, Q., et al., 2014. Aerosol oxalate and its implication to haze pollution in Shanghai, China. Chinese Science Bulletin. 59(2), 227-238. https://doi.org/10.1007/s11434-013-0009-4.

Johnson, M. S., and Meskhidze, N., 2013. Atmospheric dissolved iron deposition to the global oceans: effects of oxalate-promoted Fe dissolution, photochemical redox cycling, and dust mineralogy. Geoscientific Model Development. 6(1), 1137-1155. https://doi.org/10.5194/gmd-6-1137-2013.

Joonseon, J., and Jeyong, Y., 2005. pH effect on OH radical production in photo/ferrioxalate system. Water Research. 39(13), 2893-2900. https://doi.org/10.1016/j.watres.2005.05.014.

Kawamura, K., and Bikkina, S., 2016. A review of dicarboxylic acids and related compounds in atmospheric aerosols: Molecular distributions, sources and transformation. Atmospheric Research. 170, 140-160. https://doi.org/10.1016/j.atmosres.2015.11.018.

Kawamura, K., Imai, Y., and Barrie, L. A., 2005. Photochemical production and loss of organic acids in high Arctic aerosols during long-range transport and polar sunrise ozone depletion events. Atmospheric Environment. 39(4), 599-614. https://doi.org/10.1016/j.atmosenv.2004.10.020.

Kawamura, K., and Kaplan, I. R., 1987. Motor exhaust emissions as a primary source for dicarboxylic acids in Los Angeles ambient air. Environmental Science & Technology. 21(1), 105-110. https://doi.org/10.1021/es00155a014.

Kawamura, K., Kasukabe, H., and Barrie, L. A., 1996. Source and reaction pathways of dicarboxylic acids, ketoacids and dicarbonyls in arctic aerosols: One year of observations. Atmospheric Environment. 30(10), 1709-1722. https://doi.org/10.1016/1352-2310(95)00395-9.

Kawamura, K., Steinberg, S., and Kaplan, I. R., 2000. Homologous series of C1-C10 monocarboxylic acids and C1-C6 carbonyls in Los Angeles air and motor vehicle exhausts. Atmospheric Environment. 34(24), 4175-4191. https://doi.org/10.1016/s1352-2310(00)00212-0.

Kawamura, K., and Watanabe, T., 2004. Determination of stable carbon isotopic compositions of low molecular weight dicarboxylic acids and ketocarboxylic acids in atmospheric aerosol and snow samples. Analytical Chemistry. 76(19), 5762-5768. https://doi.org/10.1021/ac049491m.

Kawamura, K., and Yasui, O., 2005. Diurnal changes in the distribution of dicarboxylic acids, ketocarboxylic acids and dicarbonyls in the urban Tokyo atmosphere. Atmospheric Environment. 39(10), 1945-1960. https://doi.org/10.1016/j.atmosenv.2004.12.014.

Krug, E. C., and Frink, C. R., 1983. Acid rain on acid soil: A new perspective. Science. 221(4610), 520-525. https://doi.org/10.1126/science.221.4610.520.

Kundu, S., Kawamura, K., and Lee, M., 2010. Seasonal variations of diacids, ketoacids, and α-dicarbonyls in aerosols at Gosan, Jeju Island, South Korea: Implications for sources, formation, and degradation during long-range transport. Journal of Geophysical Research Atmospheres. 115(D19). https://doi.org/10.1029/2010JD013973.

Laongsri, B., and Harrison, R. M., 2013. Atmospheric behaviour of particulate oxalate at UK urban background and rural sites. Atmospheric Environment. 71(2), 319-326. https://doi.org/10.1016/j.atmosenv.2013.02.015.

Lee, A., Goldstein, A. H., Keywood, M. D., et al., 2006a. Gas-phase products and secondary aerosol yields from the ozonolysis of ten different terpenes. Journal of Geophysical Research. 111(D7). https://doi.org/10.1029/2005jd006437.

Lee, A., Goldstein, A. H., Kroll, J. H., et al., 2006b. Gas-phase products and secondary aerosol yields from the photooxidation of 16 different terpenes. Journal of Geophysical Research. 111(D17). https://doi.org/10.1029/2006jd007050.

Legrand, M., Preunkert, S., Oliveira, T., et al., 2007. Origin of C2-C5 dicarboxylic acids in the European atmosphere inferred from year-round aerosol study conducted at a west-east transect. Journal of Geophysical Research. 112(D23). https://doi.org/10.1029/2006jd008019.

Lim, H. J., Carlton, A. G., and Turpin, B. J., 2005. Isoprene forms secondary organic aerosol through cloud processing: model simulations. Environmental Science & Technology. 39(12), 4441-4446. https://doi.org/10.1021/es048039h.

Mangiante, D. M., Schaller, R. D., Zarzycki, P., et al., 2017. Mechanism of ferric oxalate photolysis. ACS Earth and Space Chemistry. 1(5), acsearthspacechem.7b00026. https://doi.org/10.1021/acsearthspacechem.7b00026.

Martinelango, P. K., Dasgupta, P. K., and Al-Horr, R. S., 2007. Atmospheric production of oxalic acid/oxalate and nitric acid/nitrate in the Tampa Bay airshed: Parallel pathways. Atmospheric Environment. 41(20), 4258-4269. https://doi.org/10.1016/j.atmosenv.2006.05.085.

Meng, J., Wang, G., Li, J., et al., 2013. Atmospheric oxalic acid and related secondary organic aerosols in Qinghai Lake, a continental background site in Tibet Plateau. Atmospheric Environment. 79(7), 582-589. https://doi.org/10.1016/j.atmosenv.2013.07.024.

Meng, J., Wang, G., Li, J., et al., 2014. Seasonal characteristics of oxalic acid and related SOA in the free troposphere of Mt. Hua, central China: Implications for sources and formation mechanisms. Science of the Total Environment. 493, 1088-1097. https://doi.org/10.1016/j.scitotenv.2014.04.086.

Millet, D. B., Baasandorj, M., Farmer, D. K., et al., 2015. A large and ubiquitous source of atmospheric formic acid. Atmospheric Chemistry & Physics. 15(11), 6283-6304. https://doi.org/10.5194/acp-15-6283-2015.

Paris, R., Desboeufs, K. V., and Journet, E., 2011. Variability of dust iron solubility in atmospheric waters: Investigation of the role of oxalate organic complexation. Atmospheric Environment. 45(36), 6510-6517. https://doi.org/10.1016/j.atmosenv.2011.08.068.

Passananti, M., Vinatier, V., Delort, A. M., et al., 2016. Siderophores in cloud waters and potential impact on atmospheric chemistry: Photoreactivity of iron complexes under sun-simulated conditions. Environmental Science & Technology. 50(17), 9324-9332. https://doi.org/10.1021/acs.est.6b02338.

Pavuluri, C. M., and Kawamura, K., 2012. Evidence for 13-carbon enrichment in oxalic acid via iron catalyzed photolysis in aqueous phase. Geophysical Research Letters. 39(3), 3802. https://doi.org/10.1029/2011gl050398.

Pavuluri, C. M., Kawamura, K., and Fu, P., 2018. Seasonal distributions and stable carbon isotope ratios of watersoluble diacids, oxoacids and α-dicarbonyls in aerosols from Sapporo: Influence of biogenic VOCs and photochemical aging. ACS Earth and Space Chemistry. https://doi.org/10.1021/acsearthspacechem.8b00105.

Pozdnyakov, I. P., Kel, O. V., Plyusnin, V. F., et al., 2008. New insight into photochemistry of ferrioxalate. The Journal of Physical Chemistry A. 112(36), 8316-8322. https://doi.org/10.1021/jp8040583.

Sedlak, D. L., Hoigné, J., David, M. M., et al., 1997. The cloudwater chemistry of iron and copper at Great Dun Fell, U.K. Atmospheric Environment. 31(16), 2515-2526. https://doi.org/10.1016/s1352-2310(96)00080-5.

Sorooshian, A., Wang, Z., Coggon, M. M., et al., 2013. Observations of sharp oxalate reductions in stratocumulus clouds at variable altitudes: organic acid and metal measurements during the 2011 E-PEACE Campaign. Environmental Science & Technology. 47(14), 7747-7756. https://doi.org/10.1021/es4012383.

Srinivas, B., M., S. M., and R., R., 2014. Atmospheric transport of mineral dust from the Indo-Gangetic Plain: Temporal variability, acid processing, and iron solubility. Geochemistry Geophysics Geosystems. 15(8), 3226-3243. https://doi.org/10.1002/2014GC005395.

Srinivas, B., Sarin, M. M., and Kumar, A., 2012. Impact of anthropogenic sources on aerosol iron solubility over the Bay of Bengal and the Arabian Sea. Biogeochemistry. 110(1-3), 257-268. https://doi.org/10.1007/s10533-011-9680-1.

Sullivan, R. C., and Prather, K. A., 2007. Investigations of the diurnal cycle and mixing state of oxalic acid in individual particles in Asian aerosol outflow. Environmental Science & Technology. 41(23), 8062-8069. https://doi.org/10.1021/es071134g.

Takahama, S., Gilardoni, S., and Russell, L. M., 2008. Single-particle oxidation state and morphology of atmospheric iron aerosols. Journal of Geophysical Research Atmospheres. 113(D22), D22202. https://doi.org/10.1029/2008jd009810.

Tanner, P. A., and Law, P. T., 2003. Organic acids in the atmosphere and bulk deposition of Hong Kong. Water Air & Soil Pollution. 142(1-4), 279-297. https://doi.org/10.1023/a:1022063925972.

Thomas, D. A., Coggon, M. M., Lignell, H., et al., 2016. Real-time studies of iron oxalate-mediated oxidation of glycolaldehyde as a model for photochemical aging of aqueous tropospheric aerosols. Environmental Science & Technology. 50(22), 12241. https://doi.org/10.1021/acs.est.6b03588.

Turekian, V. C., Macko, S. A., and Keene, W. C., 2003. Concentrations, isotopic compositions, and sources of size-resolved, particulate organic carbon and oxalate in near-surface marine air at Bermuda during spring. Journal of Geophysical Research Atmospheres. 108(D5). https://doi.org/10.1029/2002jd002053.

Vaisi-Raygani, A., Kharrazi, H., Rahimi, Z., et al., 2007. Frequencies of apolipoprotein e polymorphism in a healthy kurdish population from Kermanshah, Iran. Human Biology. 79(5), 579-587. https://doi.org/10.1016/S0045-6535(97)00228-2.

Vaïtilingom, M., Charbouillot, T., Deguillaume, L., et al., 2011. Atmospheric chemistry of carboxylic acids: microbial implication versus photochemistry. Atmospheric Chemistry & Physics. 11(16), 8721-8733. https://doi.org/10.5194/acp-11-8721-2011.

Verma, N., Satsangi, A., Lakhani, A., et al., 2017. Low Molecular Weight Monocarboxylic Acids in PM2.5 and PM10: Quantification, Seasonal Variation and Source Apportionment. Aerosol and Air Quality Research. 17(2), 485-498. https://doi.org/10.4209/aaqr.2016.05.0183.

Wang, Y., Zhuang, G., Chen, S., et al., 2007. Characteristics and sources of formic, acetic and oxalic acids in PM2.5 and PM10 aerosols in Beijing, China. Atmospheric Research. 84(2), 169-181. https://doi.org/10.1016/j.atmosres.2006.07.001.

Wang, Z., Chen, X., Ji, H., et al., 2010. Photochemical cycling of iron mediated by dicarboxylates: Special effect of malonate. Environmental Science & Technology. 44(1), 263. https://doi.org/10.1021/es901956x.

Warneck, P., 2003. In-cloud chemistry opens pathway to the formation of oxalic acid in the marine atmosphere. Atmospheric Environment. 37(17), 2423-2427. https://doi.org/10.1016/S1352-2310(03)00136-5.

Weller, C., Tilgner, A., Bräuer, P., et al., 2014. Modeling the impact of iron–carboxylate photochemistry on radical budget and carboxylate degradation in cloud droplets and particles. Environmental Science & Technology. 48(10), 5652-5659. https://doi.org/10.1021/es4056643.

Xu, J., Chen, J., Shi, Y., et al., 2019. First continuous measurement of gaseous and particulate formic acid in a suburban area of east china: Seasonality and gas-particle partitioning. ACS Earth and Space Chemistry. https://doi.org/10.1021/acsearthspacechem.9b00210.

Yang, F., Chen, H., Wang, X., et al., 2009. Single particle mass spectrometry of oxalic acid in ambient aerosols in Shanghai: Mixing state and formation mechanism. Atmospheric Environment. 43(25), 3876-3882. https://doi.org/10.1016/j.atmosenv.2009.05.002.

Yang, F., Gu, Z., Feng, J., et al., 2014. Biogenic and anthropogenic sources of oxalate in PM2.5 in a mega city, Shanghai. Atmospheric Research. 138(3), 356-363. https://doi.org/10.1016/j.atmosres.2013.12.006.

Yang, H., Yu, J. Z., Ho, S. S. H., et al., 2005. The chemical composition of inorganic and carbonaceous materials in PM2.5 in Nanjing, China. Atmospheric Environment. 39(20), 3735-3749. https://doi.org/10.1016/j.atmosenv.2005.03.010.

Yang, L., Ray, M. B., and Yu, L. E., 2008. Photooxidation of dicarboxylic acids—Part II: Kinetics, intermediates and field observations. Atmospheric Environment. 42(5), 868-880. https://doi.org/10.1016/j.atmosenv.2007.10.030.

Yu, J. Z., Huang, X. F., Xu, J., et al., 2005. When aerosol sulfate goes up, so does oxalate: implication for the formation mechanisms of oxalate. Environmental Science & Technology. 39(1), 128-133. https://doi.org/10.1021/es049559f.

Zhang, G., Lin, Q., Peng, L., et al., 2017. Insight into the in-cloud formation of oxalate based on in situ measurement by single particle mass spectrometry. Atmospheric Chemistry & Physics. 17(22), 1-39. https://doi.org/10.5194/acp-2017-763.

Zhang, G., Lin, Q., Peng, L., et al., 2018. Oxalate formation enhanced by Fe-containing particles and environmental implications. Environmental Science & Technology. https://doi.org/10.1021/acs.est.8b05280.

Zhang, T., and Croué, J.-P., 2014. Catalytic ozonation not relying on hydroxyl radical oxidation: A selective and competitive reaction process related to metal–carboxylate complexes. Applied Catalysis B Environmental. 144(144), 831-839. https://doi.org/10.1016/j.apcatb.2013.08.023.

Zhang, Y. L., Kawamura, K., Cao, F., et al., 2016. Stable carbon isotopic compositions of

low-molecular-weight dicarboxylic acids, oxocarboxylic acids, α-dicarbonyls, and fatty acids: Implications for atmospheric processing of organic aerosols. Journal of Geophysical Research: Atmospheres. 121, 3707-3717. https://doi.org/10.1002/2015JD024081.

Zhou, Y., Huang, X. H., Bian, Q., et al., 2015. Sources and atmospheric processes impacting oxalate at a suburban coastal site in Hong Kong: Insights inferred from 1 year hourly measurements. Journal of Geophysical Research Atmospheres. 120(18), 9772-9788. https://doi.org/10.1002/2015jd023531.

Zuo, Y., and Hoigne, J., 1992. Formation of hydrogen peroxide and depletion of oxalic acid in atmospheric water by photolysis of iron(III)-oxalato complexes. Environmental Science & Technology. 26(5), 1014-1022. https://doi.org/10.1021/es00029a022.

Credit author statement:

Yan-lin Zhang: Conceptualization, Methodology.

Chunyan Zhang, Chi Yang: Formal analysis, Software, Writing - Original Draft, Writing - Review & Editing.

Xiaoyan Liu: Investigation, Resources, Data Curation.

Fang Cao: Validation, Data Curation, Supervision, Project administration.

Figures

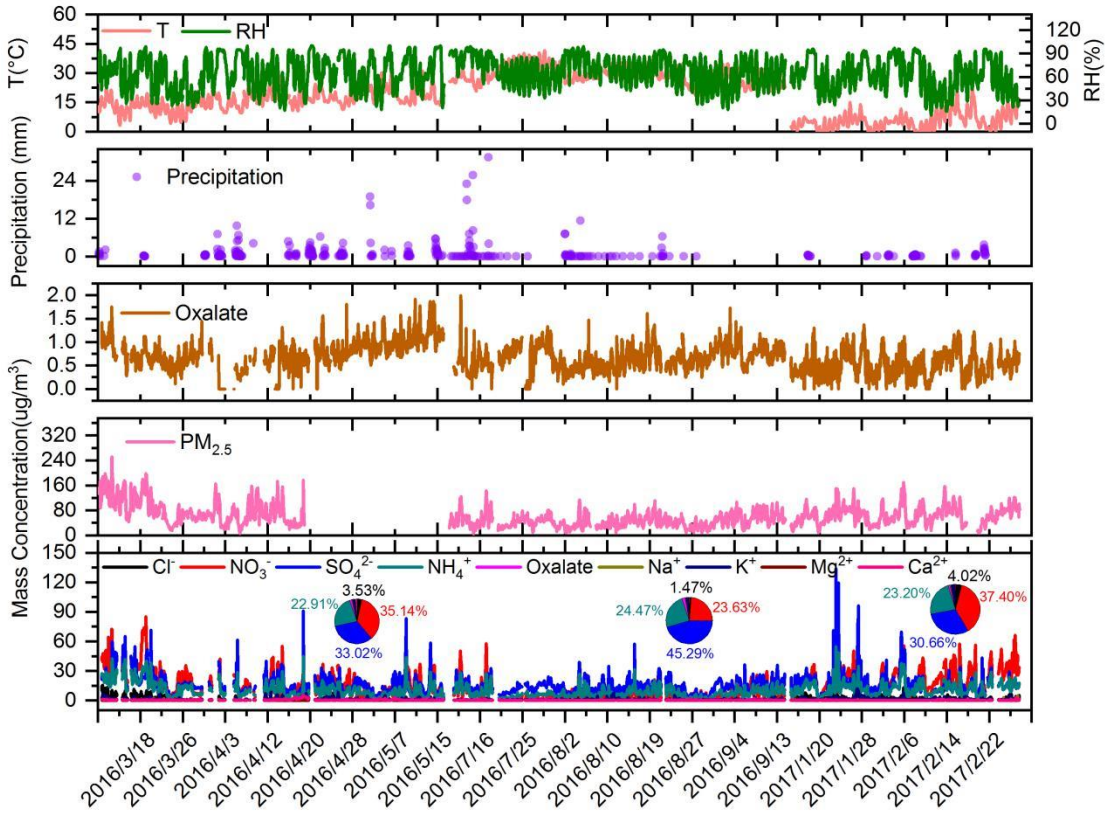

Fig. 1 Full-time series of temperature (T), relative humidity (RH), precipitation, oxalate, $PM_{2.5}$, and the concentration of water-soluble ions during sampling.

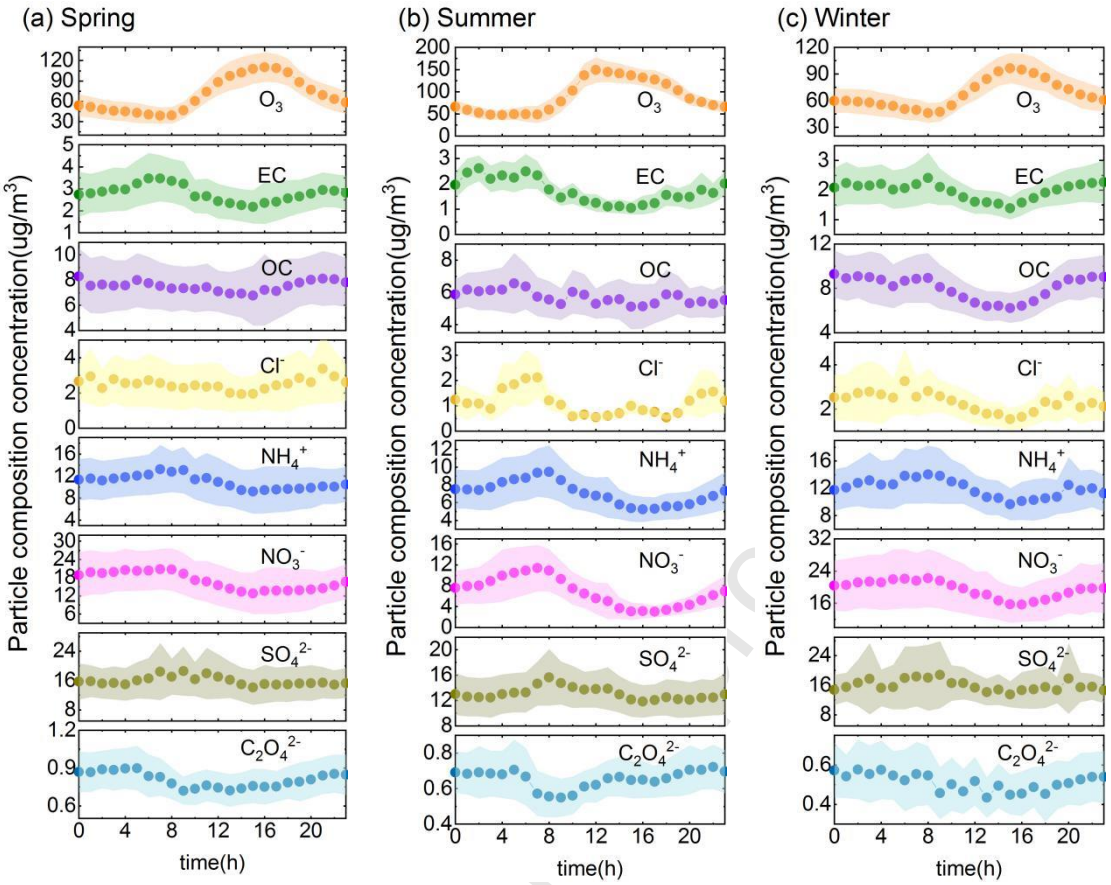

Fig. 2 The diurnal variation of O_3, OC, EC, Cl^-, SO_4^{2-}, NO_3^-, NH_4^+, and $C_2O_4^{2-}$ (shaded area corresponds to half the standard variation; x-axis is the number of the hour).

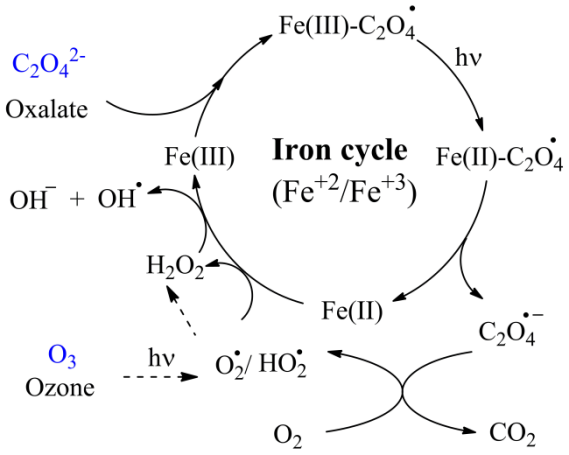

Fig. 3 The Fenton oxidation pathway of oxalate (solid line) in the atmosphere, which includes ozone oxidation (dashed line).

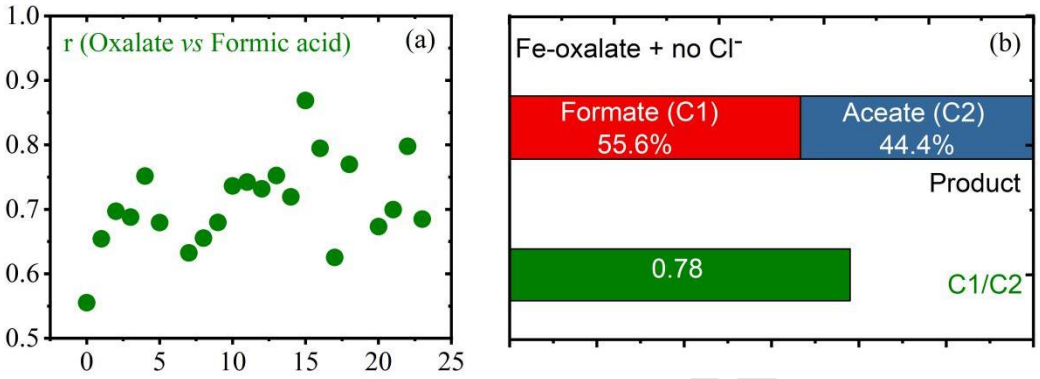

Fig. 4 (a) The diurnal variation of correlation between oxalate and formic acid (gas) in January 2017; (b) The distribution of intermediates (formate and acetate) in the oxalate-iron photochemical system.

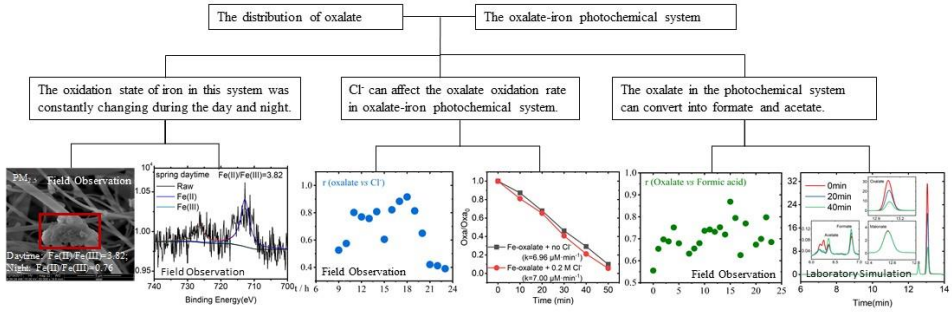

Figure. The distribution of oxalate and oxalate-iron photochemical system in the atmosphere

Highlight:

- High-resolution of oxalate showed its change was related to photochemical activities.
- The Fe(II)/Fe(III) in this observation was 3.82 during the day and 0.76 at night.
- Cl^- can affect the oxalate oxidation rate in the oxalate-iron photochemical system.
- Oxalate in the photochemical system can convert into formate and acetate slightly.

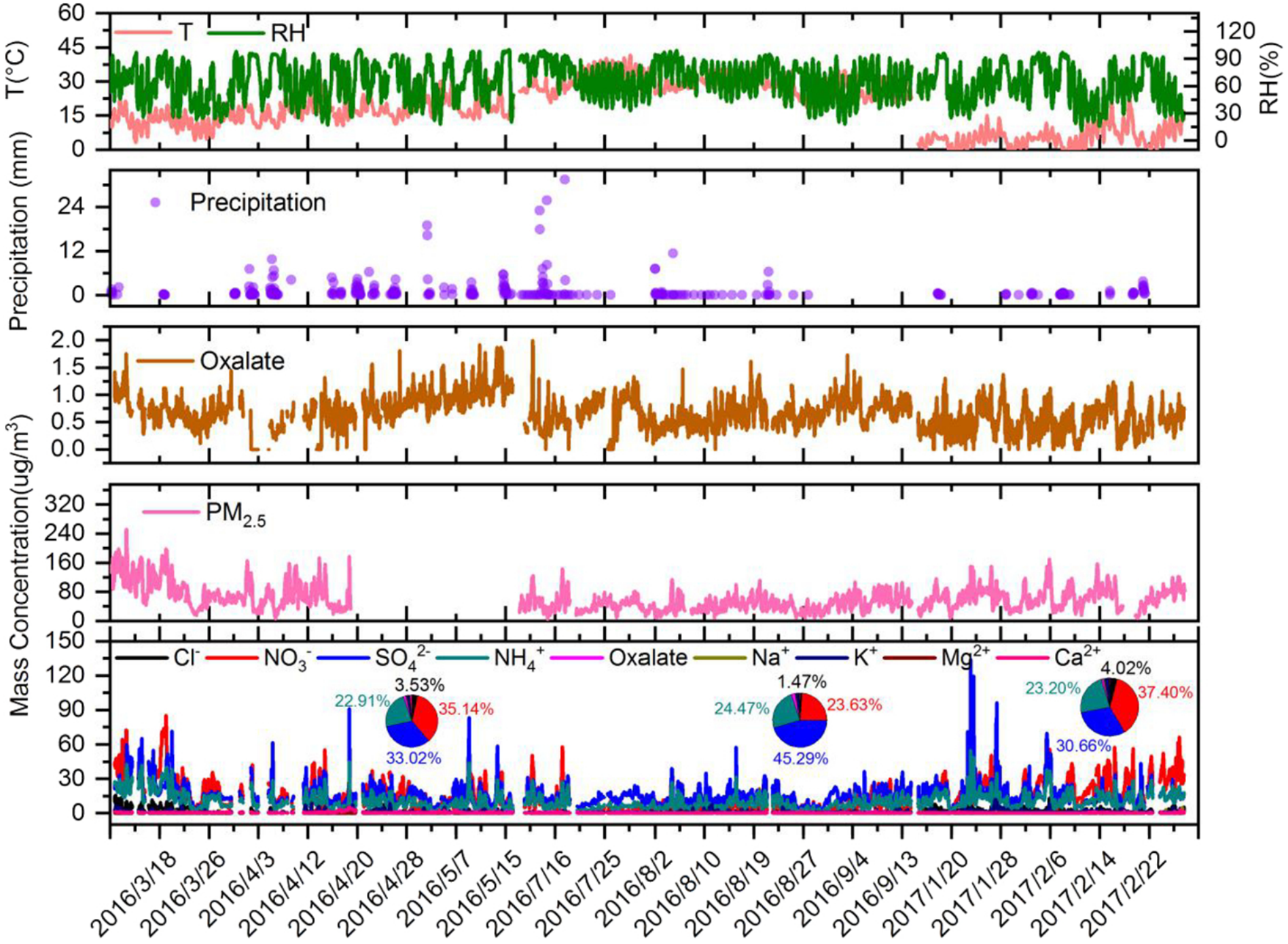
T
RH
T(°C)
RH(%)
Precipitation
Precipitation (mm)
Oxalate
PM2.5
Mass Concentration(ug/m3)
Cl-
NO3-
SO4 2-
NH4+
Oxalate
Na+
K+
Mg2+
Ca2+
3.53%
22.91%
35.14%
33.02%
1.47%
24.47%
23.63%
45.29%
4.02%
23.20%
37.40%
30.66%
2016/3/18
2016/3/26
2016/4/3
2016/4/12
2016/4/20
2016/4/28
2016/5/7
2016/5/15
2016/7/16
2016/7/25
2016/8/2
2016/8/10
2016/8/19
2016/8/27
2016/9/4
2016/9/13
2017/1/20
2017/1/28
2017/2/6
2017/2/14
2017/2/22

Figure 1

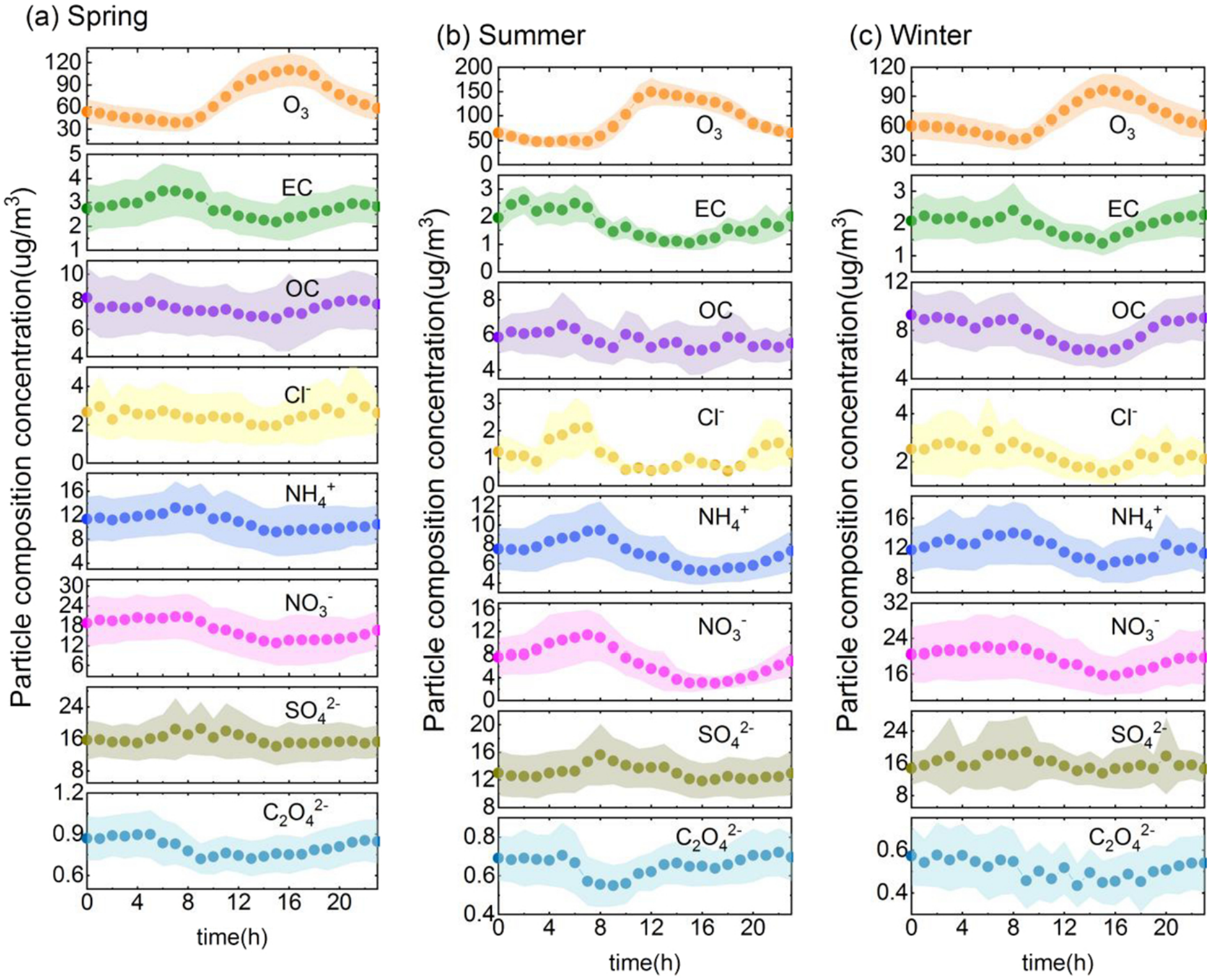
(a) Spring
(b) Summer
(c) Winter
Particle composition concentration(ug/m3)
O3
EC
OC
Cl-
NH4+
NO3-
SO4 2-
C2O4 2-
time(h)

Figure 2

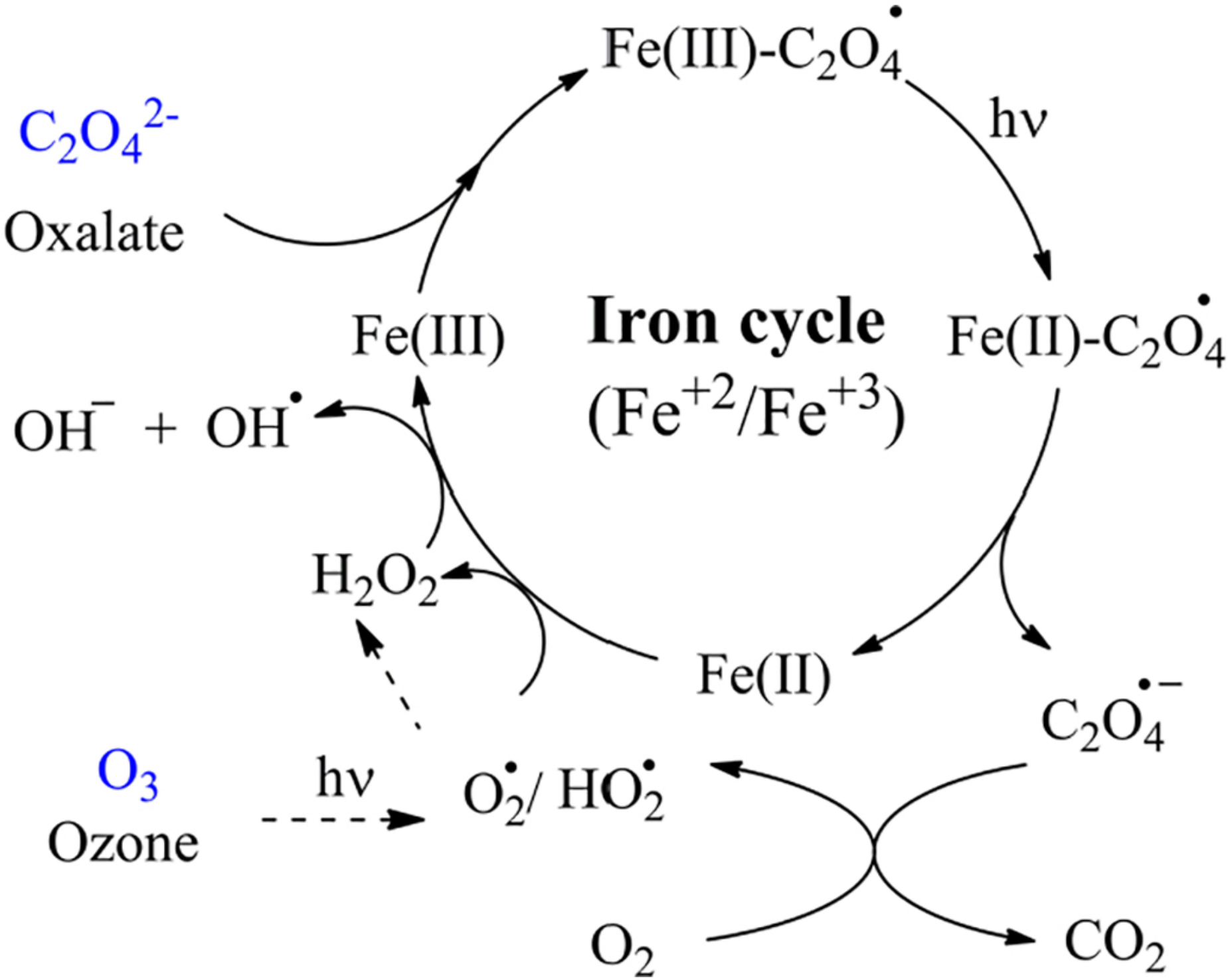
Fe(III)-C2O4•
hν
C2O4 2-
Oxalate
Iron cycle
(Fe+2/Fe+3)
Fe(III)
Fe(II)-C2O4•
OH− + OH•
H2O2
Fe(II)
C2O4•−
O3
Ozone
hν
O2•/ HO2•
O2
CO2

Figure 3

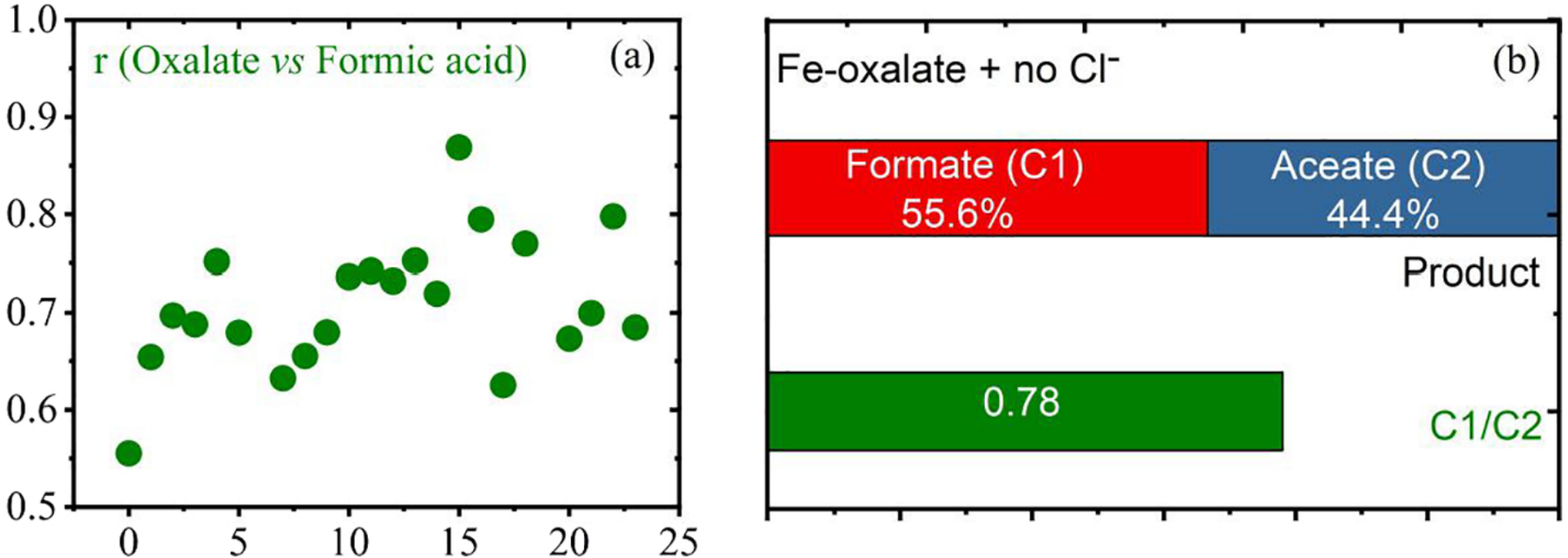
r (Oxalate vs Formic acid)
(a)
1.0
0.9
0.8
0.7
0.6
0.5
0
5
10
15
20
25
Fe-oxalate + no Cl⁻
(b)
Formate (C1)
55.6%
Aceate (C2)
44.4%
Product
0.78
C1/C2

Figure 4